Real-time monitoring of airborne molecular contamination on antireflection silica coatings using surface acoustic wave technology

Hao Zhu[1], Dongyi Ao[2], Wenting Zhang[1], Ruijie Zhang[3], Xing Shi[3], Xiaotao Zu[2], Bangji Wang[1,*], Hongyan Wang[1], Yongqing Fu[4], Yongliang Tang[1,*]

[1]School of Physical Science and Technology, Southwest Jiaotong University, Chengdu, 610031, P. R. China

[2]School of Physics, University of Electronic Science and Technology of China, Chengdu, 610054, P. R. China

[3]Nanjing Electronic Equipment Institute, Nanjing, 210007, P. R. China

[4]Faculty of Engineering and Environment, Northumbria University, Newcastle upon Tyne, NE1 8ST, UK

*Correspondence Authors:

Bangji Wang

E-mail address: bangjiw@163.com; Telephone: +86-138805492175

Yongliang Tang

E-mail address: tyl@swjtu.edu.cn; Telephone: +86-15884573263

Abstract:

Real time monitoring of contamination on antireflection (AR) silica coatings in high peak power laser systems (HPLs) is critically needed in order to avoid reductions of transmission and laser damage to optical surfaces. Herein we proposed to apply a surface acoustic wave (SAW) sensor to real-time monitor trace amounts of airborne molecular contaminants (AMCs) adsorbed on the AR silica coatings. The silica coating is found to be susceptible to AMCs because of its mesoporous structure, huge surface area and polar nature. The adsorbed AMCs caused the increased mass on the silica coating of the SAW sensor, which resulted in a significant increase of its frequency shift. The fabricated sensor showed a high sensitivity of ~-490 $mm^2ng^{-1}Hz$ and an excellent linearity vs. the areal density of adsorbed AMCs since the frequency shift of the sensor is linearly related to the change of mass of the silica coating.

Keywords: *Antireflection silica coatings; SAW sensor; Contamination; Airborne molecular contaminant*

1. Introduction

Sol-gel processed silica coatings are vastly used as thin-film antireflection (AR) coatings on the optical surfaces in high power laser systems (HPLs) because of their advantages of high laser induced damage threshold (LIDT), relatively easy deposition, and capability of large coating size [1-4]. Nevertheless, these sol-gel silica coatings are susceptible to contamination by trace volatile organic compounds because of their mesoporous structures, huge surface areas and polar nature of the silica surface [5,6].

In the HPLs, various airborne molecular contaminants (AMCs) such as plasticizers, silicon oil, lubricating oil, cutting fluid, grease, and vacuum grease released from motors, slides and other mechanisms accelerate and aggravate the contamination of the porous silica AR coating [3,5,6]. Generally, concentration of the AMCs in the system during the operation of HPLs are measured accurately several times using an *ex-situ* gas chromatograph-mass spectrometry (GC–MS). The measured AMC concentrations are ranged from 0.253 to 46.228 mg/m^3 [7]. Under these concentrations, AMCs adsorbed in the AR coatings will reduce the transmission of the laser beam. In addition, when the contamination of silica coatings reaches a certain level, the adsorbed AMC may induce a permanently physical damage to the expensive optics when exposed to the high energy density laser, thus degrading the LIDT of the silica AR coatings and the stability of the HPLs [8-10]. Therefore, it is crucial to monitor the contamination degree of the silica AR coating in real-time in order to ensure that the HPLs can work safely and stably.

Surface acoustic wave (SAW) technology has been widely applied in sensing

temperature, liquid flow, micro-force, refractive index (RI), gas, magnetic field, and electric current, etc. [11-16]. The SAW sensors have advantages of low power consumption, excellent stability, wireless control capabilities, and are extremely sensitive to the trace change of mass of the sensitive coating on the SAW device [17,18]. Our previous studies have shown that the sol-gel silica coating can be easily integrated onto the flat and smooth surface of a quartz SAW device, while SAW substrate of quartz is similar as the fused quartz of the optics [19,20]. These advantages make the SAW sensor an excellent candidate for the real-time monitoring of the trace amount of AMC residues on silica AR coating. The adsorbed AMCs on silica coating can lead to changes of the coating mass by filling the mesopores in the coating, thus causing the apparent frequency changes of the SAW devices. Nevertheless, few studies are focused on this application of the SAW sensor as far as we have searched in literatures.

In this work, we designed a SAW sensor based on a ST-cut quartz using the sol-gel AR silica as the sensitive coating for real-time monitoring of trace amounts of contaminant in silica AR coating under different environments with various AMC concentrations. The contamination sensing performance and mechanism of the SAW sensor were investigated. Results showed that the SAW sensor had excellent sensitivity, good linearity toward the AMC (e.g., the pump oil vapor).

2. Materials and methods

Commercial ST-cut quartz substrate was used for fabrication of SAW devices. Aluminum interdigitated transducers (IDTs, 30 pairs) and reflecting gratings (100 pairs) with a thickness of 200 nm were deposited on the quartz substrate using standard photolithography and lift-off processes to fabricate the SAW resonator. The IDTs and reflecting gratings had a periodicity of 16 μm. The center-to-center distance between the IDTs was ~4 mm (see Fig. 1). The resonant frequency of the resonator was measured using a network analyzer (Agilent Technologies, E8363B). The frequency reading is 200.33 MHz, the insertion loss is -9.1 dB, and the Q factor is 7433.11. The all obtained data are listed in Table 1.

Table 1 Measured parameters of SAW resonators with and without silica coating.

Samples	Pristine resonator	Resonator with silica coating
Operating frequency	200.33 MHz	198.05 MHz
Insertion loss	-9.1 dB	-19.18 dB
Q factor	7433.11	2881.32

Silica sol was prepared using a modified Stober method [21]. In a typical procedure, ethanol, Tetraethyl orthosilicate (TEOS), deionized water, and ammonia (liquid, 25 wt%) were successively added into a Bunsen flask with a molar ratio of 1:3.25:37: 0.17 under a continuous magnetic stirring. The obtained mixture was stirred at 30 ℃ for 2 h and aged for 7 days. After that, it was refluxed for 24 h to remove ammonia and finally filtered through a 0.22 μm PVDF filter. The final concentration of silica in the solution

was 3% in weight percentage.

The prepared silica sol was coated onto both the quartz surface of a SAW resonator, and the fused quartz substrates (diameter: 5 cm, thickness: 1 mm) using a spin-coating method. The latter ones were used as the reference. The thickness of silica coating can be controlled by adjusting the spinning speed. The coated SAW device and fused quartz substrates were immediately exposed to hexamethyldisilazane (HMDS) vapor, which converts most of the remaining hydroxyl groups into trimetrylsiloxy groups, and thus enhances mechanical properties of the coating [7]. As a result, mesoporous silica coatings were formed on the quartz surface of the SAW resonator and fused quartz substrates. Compared with the uncoated SAW resonator, the resonant frequency and Q factor of SAW resonator with silica coating were decreased, whereas the insertion loss was increased, and the obtained results are listed in Table 1. The coated resonator was connected to its corresponding amplifying and phase-shift circuits to fabricate a SAW sensor, as shown in Fig. 1.

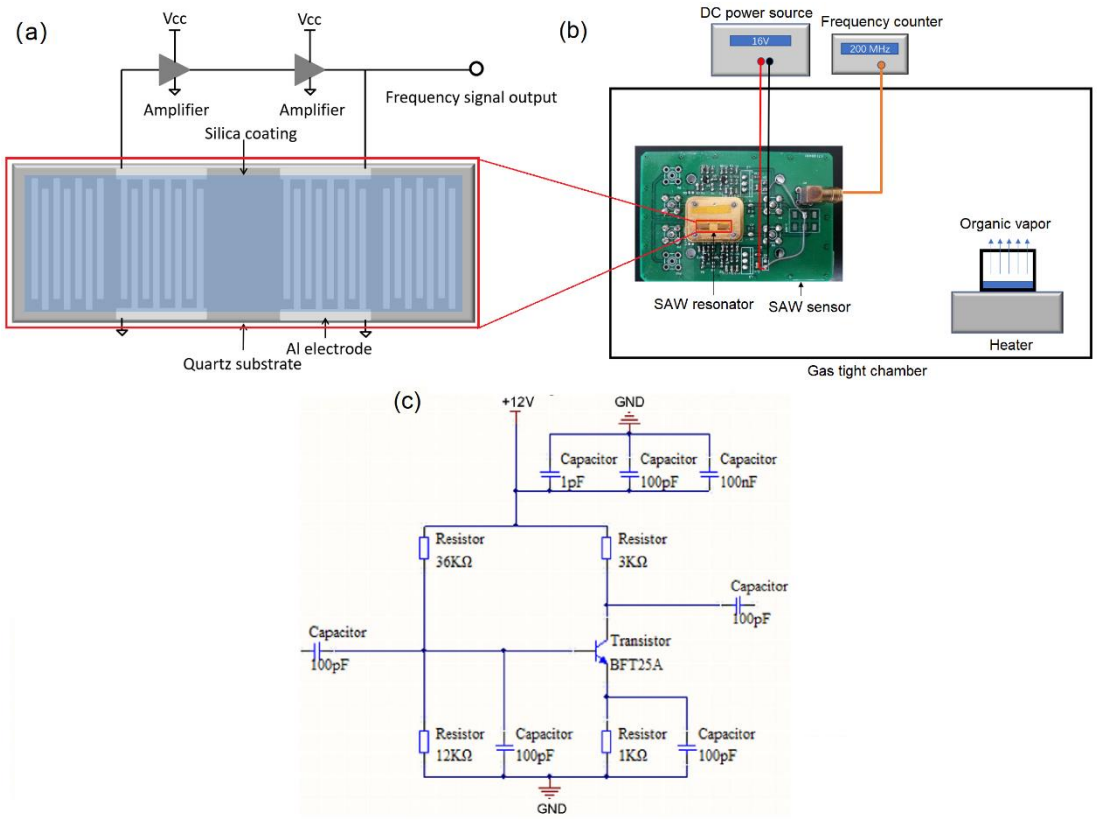

Fig. 1 (a) The schematic diagram of a SAW sensor; (b) Experimental setup for AMC sensing measurement; (c) The detail parameters of the components used in the amplifiers in (a).

Different lubricants are widely used in the HPLs, and they are one of the most critical contaminants which influence the HPLs [3,22]. Therefore, in our experiment, the vacuum pump oil (obtained from China Academy of Engineering Physics) was chosen as the measured contaminant, and its density is about 0.85 g/ml. The experiments were carried out in a cleanroom with controlled temperature and humidity. Before the experiment, an airtight chamber and other equipment used in the experiment were cleaned with high pressure spray and ultrasonic cleaning method to remove any contaminants.

The experimental set-up for AMC sensing is illustrated in Fig. 1 (right panel). In

the gas chamber, a weighing bottle containing a certain amount of vacuum pump oil (the vacuum pump oil was transferred into the bottle using a precision pipette) was put on a magnetic stirrer with a precise control of temperature. The relative humidity in the test chamber was kept at 40% to avoid the influence of humidity. The fabricated SAW sensor and three fused quartz substrates with the silica coating on both sides were mounted away from the magnetic stirrer to avoid the influence of its temperature. During the tests, different amounts of vacuum pump oil were fully evaporated into AMC (vacuum pump oil vapor) at 180 ℃, which leads to different AMC concentrations in the chamber, thus the different contamination degrees of the silica AR coatings. The response of the SAW sensor is defined as $\Delta f = f_s - f_0$, where f_s is the oscillating frequency of the sensor with contaminated coating, and f_0 is the oscillating frequency of the sensor with newly made coating, respectively. The frequency was recorded using a frequency counter (HP 5385A, Agilent). The fused quartz substrates were weighed using a microbalance (XP56, METTLER TOLEDO) before and after contamination in order to evaluate the areal density of the pump oil adsorbed on the silica coating.

The silica coating was analyzed using the X-ray diffraction (XRD, Bruker AXS D8 ADVANCE X-ray diffractometer) with a Cu Kα (λ = 1.5418 Å) radiation source, operated at 40 kV and 40 mA. A Fourier Transform Infrared spectroscope (FTIR, Nicolet IS 10) with a wavelength range of 400–4000 cm^{-1} was used to obtain the infrared transmission spectra of silica coatings. Microstructure and morphologies of the silica AR coatings were characterized using a scanning electron microscope (SEM, JEOL JSM-7001F) operated at 15 kV. The surface area of the coating was evaluated

based on the Brunauer–Emmett–Teller (BET) method using the instrument of ASAP-2020, with the adsorption branch in a relative pressure range from 0.01 to 1. The pore size distribution was derived from the adsorption branches of the isotherms using the Barrett–Joyner–Halenda (BJH) model.

3. Results and discussions

3.1. Characterization results of the silica coating

Figs. 2(a) and 2(b) show the SEM images of surface morphologies for the silica coatings on both SAW resonator and fused quartz substrate. These two coating surfaces have similar morphology, which is composed of nanoparticles with an average diameter of ~15 nm. Mesopores with an average diameter of tens of nanometers can be found on the surface, indicating the porous nature of the silica coatings. The cross-sectional images of these two coatings are shown in the insets, which indicate the thicknesses of these coatings are ~80 nm. These results indicate that these two coatings have similar microstructure and thickness.

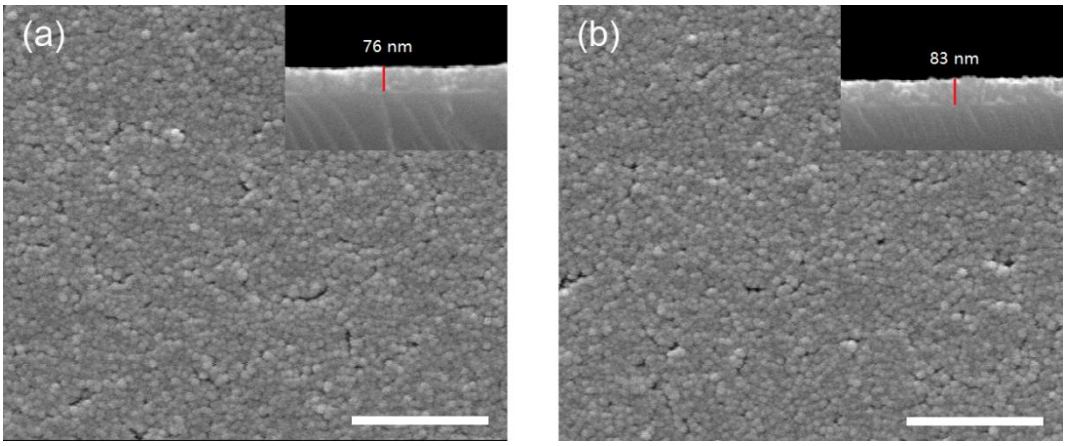

Fig. 2 SEM images of the silica coating. Inset is the sectional view of the coating. Scale bar is 500 nm.

The specific surface areas and pore distribution of the silica powders obtained from the as-deposited coatings are shown in Fig. 3(a). The measured BET surface area of silica obtained from the coating is 1519.9 m^2/g. Fig. 3(b) shows that the pore size of the silica material ranges from 3 to 9 nm. The total pore volume is 1.43 cm^3/g, and the

calculated average pore diameter is 4.9 nm. These results confirm the mesoporous microstructure of the silica material.

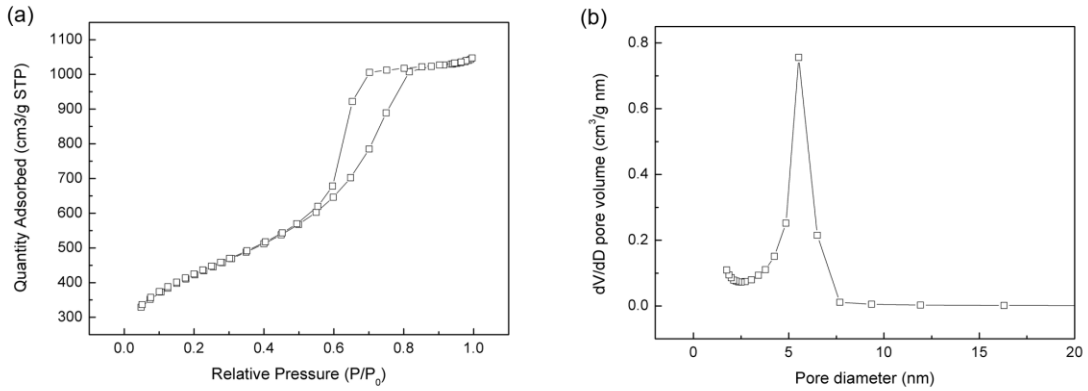

Fig. 3 (a) N_2 adsorption and desorption isotherms and (b) pore distributions of the silica sample.

XRD pattern of the silica film shown in Fig. 4(a) reveals a broad peak at about 23°, which is the typical character of amorphous SiO_2. The typical FTIR spectrum of silica coating is presented in Fig. 4(b). In the high wave number spectral range, a broad peak between 3600 and 2800 cm^{-1} can be observed, which can be assigned to fundamental stretching vibration modes of OH hydroxyl groups (free or bounded) [23]. The band at 1630 cm^{-1} is associated to molecular water, and the band at ~960 cm^{-1} is attributed to stretching mode of non-bridging oxygen atoms, e.g., Si-OH [23]. Various bands at 427, 790, and 1070 cm^{-1} are associated with the transverse optical (TO) modes of silica. The shoulder at 1210 cm^{-1} is associated with the longitudinal optical LO3 mode of silica while the shoulder at 3650 cm^{-1} is associated with the SiOH stretching mode [23]. The polar hydroxyl groups, together with mesoporous structure are believed to make sol-gel silica coating susceptible to contaminants.

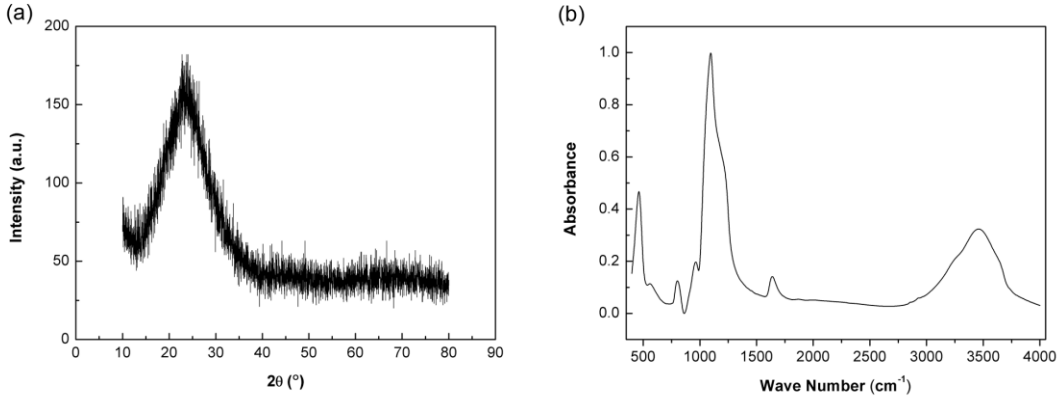

Fig. 4 XRD pattern (a) and FTIR spectrum (b) of the silica coating.

3.2. Stability, sensitivity and temperature coefficient of the fabricated SAW sensor

The fabricated SAW sensor with the fresh silica AR coating was put in a constant temperature (27 °C) and humidity (RH=40%) test chamber to evaluate its stability. As shown in Fig. 5(a), its working frequency fluctuated within ±20 Hz (the minimum resolution of the HP 5385A frequency counter is 10 Hz) in a period of 10000 s, indicating its excellent stability in a constant environmental condition. The temperature sensitivity of the sensor was investigated by changing the temperature of the test chamber from 27 °C to 60 °C. Results presented in Fig. 5b indicate the working frequency of the sensor is shifted non-linearly with the temperature, and their relationship can be fitted with a 2nd polynomial, as shown in Fig. 5b. When temperature is changed from 27 °C to 60 °C, the frequency is shifted by -24000 Hz.

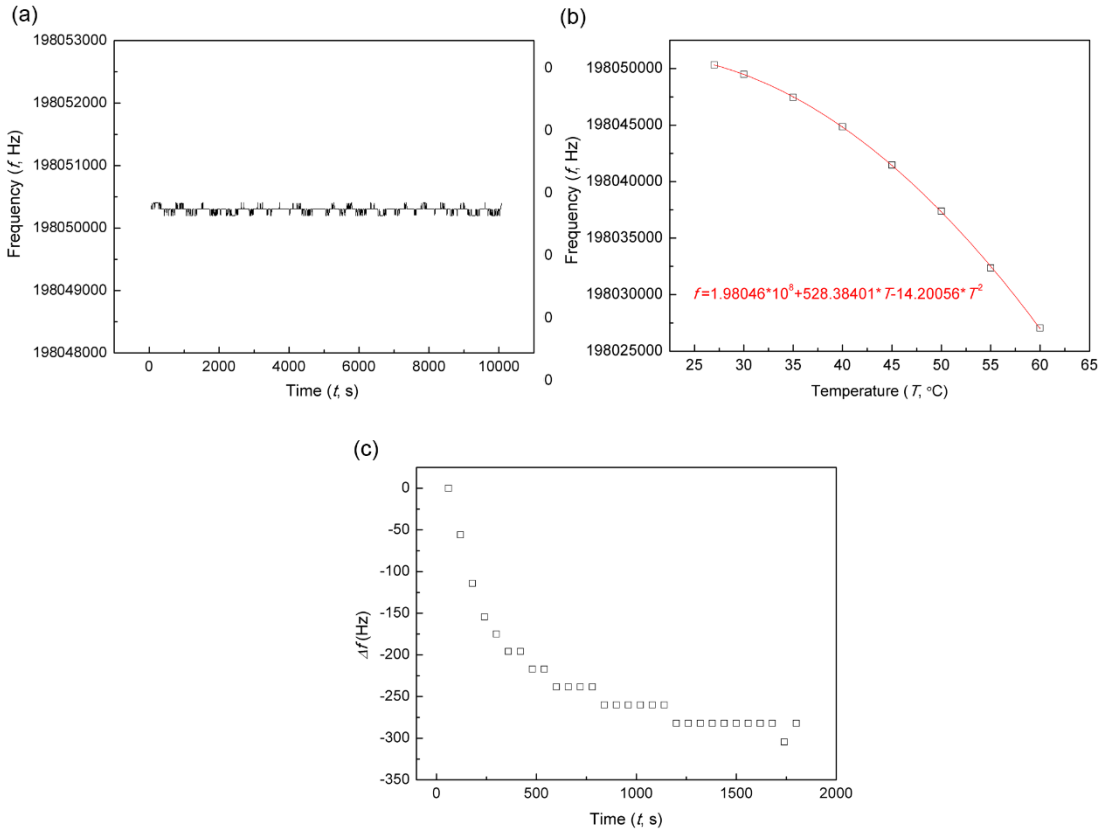

Fig. 5 (a) The dynamic working frequency of the sensor in a constant environment; (b) The dynamic working frequency of the sensor with the temperature varying from 27 ° C to 60 °C; (c) The calculated temperature-induced frequency shift of the SAW sensor caused by the evaporation process.

As discussed above, the evaporation process of the pump oil could induce the heating of the SAW sensor, thus inducing a frequency shift. To investigate the influence of the evaporation process on the operating temperature and the working frequency of the SAW sensor, a temperature probe was mounted near the SAW resonator to measure operating temperature of the sensor during the evaporation process. The operating temperature was increased from 27 ℃ to 28.2 ℃ during the evaporation process. By using the fitted equation as shown in Fig. 5(b), the temperature-induced frequency shift

caused by the evaporation process can be calculated and the results are shown in Fig. 5(c). Clearly, the frequency shift caused by the temperature was less than -350 Hz.

To evaluate the sensitivity of the SAW sensor toward the adsorption of pump oil, a drop (4 μl) of acetone diluted pump oil (0.05 vol.%) was directly dripped onto the SAW resonator. After the vaporization of acetone, certain amount (~1.7 μg) of pump oil was left on the silica coating. By repeating the process, the increased amount of pump oil can be introduced onto the silica coating. Fig. 6(a) shows the dynamic response of the SAW sensor, and when a drop of acetone was dripped onto the device, the signal of SAW sensor immediately disappeared since most wave energy was dissipated by the liquid acetone. The signal of the SAW sensor was gradually recovered due to the vaporization of acetone. Meanwhile, a negative shift of working frequency caused by the left pump oil can be observed. With adding each new drop, the working frequency of the sensor is kept decreasing as shown in Fig. 6(a). By conducting the experiments using three different sensors with the same silica coating, the relationship between the areal density of pump oil residue on the silica coating and frequency shift of the SAW sensor were obtained and the results are shown in Fig. 6(b). Obviously, the frequency shift (Δf) was linearly related with the areal density of pump oil (σ), and the slope was -490 $mm^2ng^{-1}Hz$, i.e. the sensitivity of the sensor toward pump oil adsorbed in the silica coating was -490 $mm^2ng^{-1}Hz$.

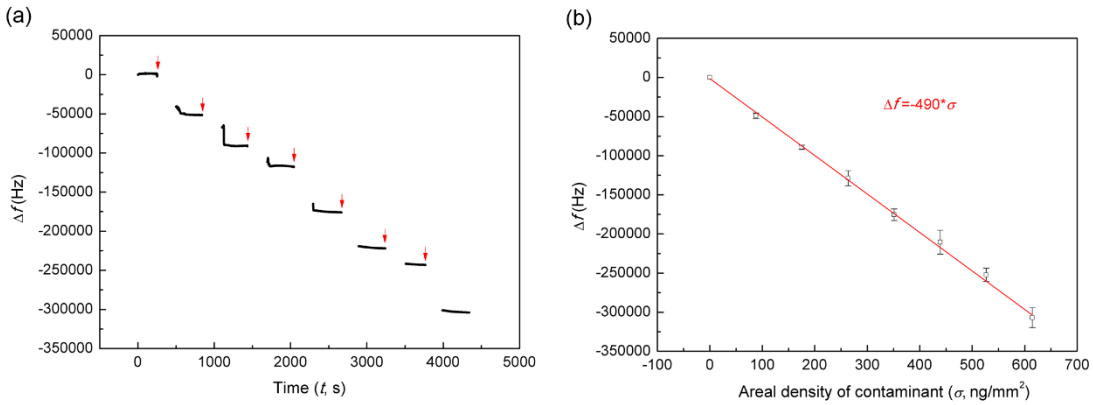

Fig. 6 (a) Dynamic response of the SAW sensor toward drops of acetone containing the pump oil, the red arrows indicate where the acetone was dripped; (b) Relationship between the areal density of pump oil (σ) residue on the silica coating and the response of the sensor (Δf).

The relationship between the frequency shift and the change of the areal density of the sensitive film has been reported to follow the theoretical equation as below [24,25],

$$\Delta f = c_m \times f_0^2 \times \Delta\rho_s \quad (1)$$

where c_m is a substrate material constant of ST-cut quartz substrate, and $\Delta\rho_s$ is the variation of areal density of the sensitive coating. Based on this equation, the responses of frequency shift and the areal density of contaminant adsorbed should be linearly related. This is in a good agreement with the experimental result (Fig. 6(b)).

3.3. Sensing performance of the SAW sensor toward the AMC (pump oil vapor)

Fig. 7(a) shows the dynamic frequency responses of the sensor during the evaporation processes of different amounts of vacuum pump oil by directly subtracting the temperature-induced frequency shift (Fig. 5(c)) from the total frequency shift. Obviously, the sensor shows negative responses of frequency shifts during the evaporation process. These negative responses were mainly caused by the adsorbed

AMC, which increased the areal density of the silica coating by filling the mesopores in the coating. In addition, the responses to the evaporation time is nonlinear due to non-uniform vaporization of pump oil during the evaporation process. In the first several minutes of the evaporation process, the frequency was only slightly shifted, indicating that the amount of the evaporated AMC was insignificant. Thereafter, the sensor exhibited relatively strong frequency shifts since the AMC concentration in the chamber was increased rapidly. When the pump oil in the bottle was fully evaporated, the response became stable because of the AMC concentration reached a constant value.

Fig. 7(a) reveals that the response of the sensor was increased with the AMC concentration, because more contaminants were evaporated and adsorbed onto the silica coating. When the concentrations of AMC were 10.8 mg/m^3 and 87 mg/m^3, the responses were -2310 Hz and -9800 Hz, respectively. The relationship between the response and the AMC concentration is nonlinear as shown in Fig. 7(b). By using the fitting equation in Fig. 6(b), the amount of AMC residues on silica coating can be calculated and the results are shown in Fig. 7(c). A polynomial fitting was applied to estimate the amount of AMC adsorbed on silica coating with respective to the concentration of AMC, and the obtained result are presented in Fig. 7(c). By using the fitting equations in Fig. 6(b) and Fig. 7(c), the concentration of the AMC in the testing chamber and the amount of AMC adsorbed on the silica film can be determined based on the measured frequency shift of the SAW sensor.

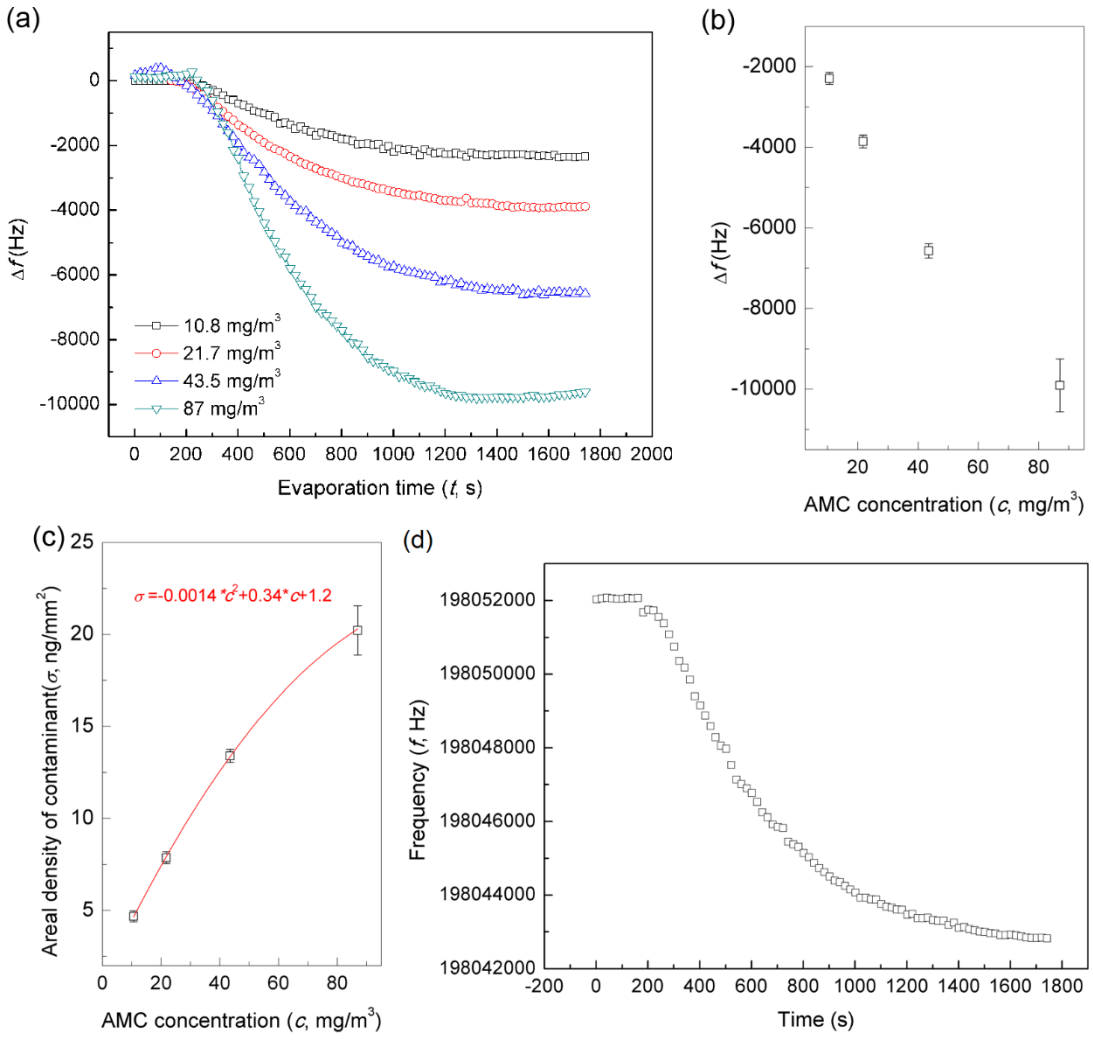

Fig. 7 (a) Dynamic responses of the sensor during the evaporation processes of vacuum pump oil of different amounts; (b)The response as a function of the AMC concentration; (c) The areal density of the contaminant adsorbed on the silica coating as a function of the AMC concentration; (d) Dynamic response of the sensor with the cleansed resonator during the evaporation processes of vacuum pump oil, and the AMC concentration is 87 mg/m^3.

To confirm the above sensing principle, three fused quartz substrates with the silica coatings in the test chamber were together weighted before and after the evaporation processes with the different AMC concentrations of 10.8, 21.7, 43.5, 87 mg/m^3. The

total increased weights of the three substrates after the evaporation processes were 64, 108, 181, 272 ug. Assuming the adsorbed vacuum pump oil is covered uniformly on the surface of the substrates, the areal density value of the adsorbed pump oil can be obtained using the increased weight divided by the surface area of the three substrates: i.e., 1964 $mm^2 \times 3 \times 2$ (three pieces of substrates with both sides coated). The obtained values are 5.4 ng/mm^2, 9.2 ng/mm^2, 15.4 ng/ mm^2, 23.1 ng/mm^2, respectively. These results are in good agreements with the results derived from the response of SAW sensor, as shown in Fig. 7(c), which further confirms that the fabricated SAW sensor is able to monitor precisely the contamination of the silica coating quantitatively.

After the evaporation processes, the sensor was exposed to the ambient environment. There was no significant recovery of the frequency can be observed, indicating most of the contaminant was left on the silica coating. To investigate the re-usability of the fabricated sensor, the contaminated SAW resonator was cleaned by acetone, ethanol and deionized in an ultrasonic bath, successively, before bonded back to the equivalent circuit to form the SAW sensor again. The working frequency of the cleaned sensor was measured and the changes of frequency signals for another evaporation process was recorded. As shown in Fig. 7(d), the sensor shows the similar working frequency compared with the pristine one, indicating that the pump oil evaporated onto the silica coating can be easily removed by the cleaning process and the silica coating was stable during the contamination and washing cycle. Besides, the sensor exhibited a similar response toward the AMC (87 mg/m^3) during the repeated

evaporation process. The above result confirms the excellent re-usability of the fabricated sensor toward AMC.

Conclusions

In this paper, we have successfully fabricated a SAW sensor for real-time monitoring the areal density of AMC (e.g., evaporated pump oil vapor) adsorbed in antireflection silica coating, which is commonly used in HPL systems. The silica coating is found to be susceptible to AMC contamination because of its mesoporous structures, huge surface area and polar nature of the silica surface. The adsorbed AMC will cause an increased mass of the silica coating on SAW device, which results in negative frequency shift of the sensor. The negative frequency shift is linearly related to the areal density of AMC adsorbed. The sensor's sensitivity is ~-490 $mm^2ng^{-1}Hz$ toward AMC adsorbed, and has good stability and reusability as well.

Acknowledgements

This work was supported by the Fundamental Research Funds for the Central Universities (2682019CX68), the Scientific Research Foundation of SWJTU (A1920502051907-2-032), the National Natural Science Foundation of China (51902272) and the NSAF Joint Foundation of China (U1630126 and U1230124).

References

[1] X. Wang, J. Shen, A review of contamination-resistant antireflective sol-gel coatings, J. Sol-Gel Sci. Techn. 61 (2012) 206-212.

[2] X. Li, L. Zou, G. Wu, J. Shen, Laser-induced damage on ordered and amorphous sol-gel silica coatings, Opt. Mater. Express 4 (2014) 2478-2483.

[3] R. Pareek, M.N. Kumbhare, C. Mukherjee, A.S. Joshi, P. K. Gupta, Effect of oil vapor contamination on the performance of porous silica sol-gel antireflection-coated optics in vacuum spatial filters of high-power neodymium glass laser, Opt. Eng. 47 (2008) 023801.

[4] J. Huang, Y. Liu, Y. Cao, Q. Liu, J. Shen, X. Wang, Durable silica antireflective coating prepared by combined treatment of ammonia and KH570 vapor, J. Coat. Technol. Res. 16 (2019), 615-622.

[5] X. Li, J. Shen, The stability of sol–gel silica coatings in vacuum with organic contaminants, J. Sol-Gel Sci. Techn. 59 (2011) 539-545.

[6] F.Y. Genin, A. Salleo, A.K. Burnham, J. De Yoreo, K. Bletzer, J.R. Lukes, Laser Damage of Contaminated Anti-Reflective Sol-Gel Coatings. In LLNL document server, Abstract Prepared for the 1999 International Symposium on Optical System Design and Production.

[7] G. Zhou, L. Niu, Y. Jiang, H. Liu, X. Xie, H. Yan, L. Yan, J. Liu, J. Chen, X. Miao, H. Zhou, X. Jiang, H. Lv, Sensing of airborne molecular contaminants based on microfiber coupler with mesoporous silica coating, Sens. Actuat. A-Phys. 287 (2019)1-7.

[8] K. Bien-Aime, C. Belin, L. Gallais, P. Grua, E. Fargin, J. Neauport, I. Tovena-Pecault, Impact of storage induced outgassing organic contamination on laser induced damage of silica optics at 351nm, Opt. Express 17 (2009)18703-18713.

[9] L. Yang, X. Xiang, X.X. Miao, Z.J. Li, X.D. Yuan, G.R. Zhou, H.B. Lv, X.T. Zu, Influence of oil contamination on the optical performance and laser induced damage of fused silica, Opt. Laser Technol. 75 (2015) 76-82.

[10] X. Ling, Y. Zhao, J. Shao, Z. Fan, Effect of two organic contamination modes of laser-induced damage of high reflective films in vacuum, Thin Solid Films 519 (2010) 296-300.

[11] J. Kim, R. Luis, M.S. Smith, J.A. Figueroa, D. C. Malocha, B. H. Nam, Concrete temperature monitoring using passive wireless surface acoustic wave sensor system, Sens. Actuat. A-Phys. 2015 224 (2015) 31-139.

[12] J. Kondoh, N. Ohashi, Measurements of blood coagulation using digital micro-fluidic system based on surface acoustic wave devices. In 2015 International Conference on Quality in Research (QiR), IEEE (2015, August) 9-22.

[13] S. Okuda, T. Ono, Y. Kanai, T. Ikuta, S. Shimatani, S. Ogawa, K. Maehashi, K. Inoue, K, Matsumoto, Graphene surface acoustic wave sensor for simultaneous detection of charge and mass, ACS sensors 3 (2018) 200-204.

[14] Y. Jia, W. Wang, X. Xue, S. He, Y. Liang, Development of Surface Acoustic Wave Magnetic Field Sensor Incorporating with FeCo Dot Film. In 2018 IEEE International Ultrasonics Symposium (IUS). IEEE (2018, October)) 1-3.

[15] Y. Tang, X. Xu, S. Han, C. Cai, H. Du, H. Zhu, X. Zu, Y. Fu, ZnO-Al_2O_3 nanocomposite as a sensitive layer for high performance surface acoustic wave H_2S gas sensor with enhanced elastic loading effect, Sens. Actuators. B: Chem. 304 (2020) 127395.

[16] Y. Tang, D. Li, D. Ao, Y. Guo, M.B. Faheem, B. Khan, X. Zu, S. Li, Highly sensitive surface acoustic wave HCl gas sensors based on hydroxyl-rich sol-gel AlO_xOH_y films, Mater. Chem. Phys. 239 (2020) 122026.

[17] A.J. Ricco, S.J. Martin, T.E. Zipperian, Surface acoustic wave gas sensor based on layer conductivity changes, Sens. Actuators 8 (1985) 319–333.

[18] Jr D.S. Ballantine, H. Wohltjen, Surface acoustic wave devices for chemical analysis, Anal. Chem. 61 (1989) 704A-715A.

[19] Y. Tang, Z. Li, J. Ma, L. Wang, J. Yang, B. Du, Q. Yu, X. Zu, Highly sensitive surface acoustic wave (SAW) humidity sensors based on sol-gel SiO_2 films: Investigations on the sensing property and mechanism, Sens. Actuators. B: Chem. 215 (2015) 283-291.

[20] Y. L. Tang, D. Y. Ao, W. Li, X. T. Zu, S. Li, Y. Q. Fu, NH_3 sensing property and mechanisms of quartz surface acoustic wave sensors deposited with SiO_2, TiO_2, and SiO_2-TiO_2 composite films, Sens. Actuators. B: Chem. 254 (2018) 1165-1173.

[21] W. Stöber, A. Fink, E. Bohn, J. Colloid Interface Sci. 26 (1968) 62–69.

[22] Z. Wei, Z. Song, Y. Yu, X. Zhang, Z. Meng, Inline contaminants detection with optical microfiber in high-power laser system. In International Symposium on

Photoelectronic Detection and Imaging 2013: Micro/Nano Optical Imaging Technologies and Applications 8911 (2013, August) 891104

[23] N. Primeau, C. Vautey, M. Langlet, The effect of thermal annealing on aerosol-gel deposited SiO_2 films: a FTIR deconvolution study, Thin Solid Films 310 (1997) 47–56.

[24] V.B. Raj, H. Singh, A.T. Nimal, M.U. Sharma, M. Tomar, V. Gupta, Distinct detection of liquor ammonia by ZnO/SAW sensor: study of complete sensing mechanism, Sensor. Actuat. B-Chem. 238 (2017) 83–90.

[25] D.S. Ballantine Jr., S.J. Martin, A.J. Ricco, G.C. Frye, H. Wohltjen, R.M. White, E.T.Zellers, Acoustic Wave Sensors: Theory, Design, and Physico-Chemical Applications, Academic Press, San Diego, 1997.